NASA TECHNICAL MEMORANDUM NASA TM-77983

EFFECT OF VOLUME FRACTION AND SIZE OF FINE GAMMA-PRIME PARTICLES ON RAISING THE CREEP STRENGTH OF A DS NICKEL-BASE SUPERALLOY

Lin, D.L.; Yao, D.L.; Lin, X.J.; Sun, C.Q.

Translation of Acta Metallurgica Sinica, Vol. 18, No. 1, Beijing China, February 1982, pp. 104-114.

NATIONAL AERONAUTICS AND SPACE ADMINISTRATION
WASHINGTON, D.C. 20546

FEB 1986

STANDARD TITLE PAGE

1. Report No. NASA TM-77983	2. Government Accession No.	3. Recipient's Catalog No.
4. Title and Subtitle EFFECT OF VOLUME FRACTION AND SIZE OF FINE-GAMMA PRIME PARTICLES ON RAISING THE CREEP STRENGTH OF A DS NICKEL-BASE SUPERALLOY		5. Report Date 6. Performing Organization Code
7. Author(s) Lin, D.L.; Yao, D.L.; Lin, X.J.; Sun, C.Q.		8. Performing Organization Report No. 10. Work Unit No.
9. Performing Organization Name and Address Leo Kanner Associates Redwood City, CA 94063		11. Contract or Grant No. 13. Type of Report and Period Covered Translation
12. Sponsoring Agency Name and Address National Aeronautics and Space Administration, Wash., D.C. 20546		14. Sponsoring Agency Code

15. Supplementary Notes
Translation of:
Acta Metallurgica Sinica, Vol. 18, Feb., 1982, pp. 104-114.
(A82-33045)

16. Abstract

The creep behavior of a directionally solidified nickel-base superalloy, DSK3, has been investigated as a function of the volume fraction and size of the gamma-prime phase at 760 and 950°C. The dislocation structure and morphology of gamma-prime was examined by transmission electron microscopy at the primary, secondary and tertiary creep stages at 73.8 kgf/sq mm. Experimental results are described in terms of a high temperature creep model in the range of temperatures and applied stresses where shearing of the gamma-prime phase does not control the straining process.

17. Key Words (Selected by Author(s)) "Unclassified-Unlimited"	18. Distribution Statement		
19. Security Classif. (of this report) Unclassified	20. Security Classif. (of this page) Unclassified	21. No. of Pages 23	22.

EFFECT OF VOLUME FRACTION AND SIZE OF FINE GAMMA-PRIME PARTICLES ON RAISING THE CREEP STRENGTH OF A DS NICKEL-BASE SUPERALLOY

D.L.Lin and D.L.Yao

Shanghai Jiaotong University
Shanghai, People's Republic of China

X.J.Lin

Shanghai Institute of Iron and Steel
Shanghai, People's Republic of China

C.Q. Sun

Institute of Aeronautical Materials
Shanghai, People's Republic of China

I. Introduction /104

By directionally solidifying a gamma prime-Ni_3 (Al, Ti) phase strengthened high strength casted nickel-base superalloy, we were able to obtain parallel columnar crystals and this raised to a great extent the alloy's longitudinal (the main stress axis was parallel to the growth direction of the columnar crystals) plasticity, creep strength, rupture life and thermal fatigue etc. superalloy comprehensive mechanical performances [1-2]. Suitable high temperature solid solution aging treatment (for example, 1210-1230°C, 4h, air cooling + 900°C, 16-32h, air cooling) can further raise by multiples the creep /105 strength of a directionally solidified alloy and lengthen its rupture life. This is because the high temperature solid solution trestment causes relatively large cast gamma-prime particles to dissolve. During the later cooling, uniform, dispersed and fine gamma-prime particles were again extracted and thus brought about alloy strengthening results [2-4]. Jackson et al [5] obtained the fine gamma-prime phase and were able to raise the high temperature (982°C) rupture life three fold. One of the authors of this paper systematically researched the effects of the high temperature solid solution treatment on raising the medium temperature (760°C) creep strength of the directionally solidified K17G nickel-base superalloy [6] and

discovered that second stage creep rate $\dot{\varepsilon}$ changed with the size a, center-to-center separation L and volume fraction v_f of the fine gamma-prime phase. He also found that $\dot{\varepsilon} \propto \frac{L_2}{a}$ or $\dot{\varepsilon} \propto a/v_f^{2/3}$. This paper further systematically researches the relationship between the high temperature (1100-1270°C) solid solution treatment, the quantity and size of the directionally solidified K3 nickel-base superalloy's gamma-prime phase and the creep strength and rupture life of the alloy. It also used a transmission electron microscope to observe the dislocation substructure changes of the alloy after medium temperature (760°C) and high temperature creeping as well as the interaction between it and the gamma-prime phase. We also proposed a strengthening mechanism and creep model for the alloy.

II. Test Method

The material used in this paper is K3 high strength cast nickel-base superalloy and its mother alloy composition (wt-%) is as follows:

C	Cr	Co	W	Mo	Al	Ti	B	Zr	Ce	Ni
0.09	10.92	4.91	5.11	4.27	5.50	2.58	0.015	0.009	0.01 0.03	remainder

We used the power lowering method for the directional solidification and it was carried out in a vacuum induction furnace. The size of the directional test piece was 100x42x14mm and the lower half of the directional test piece was machined into a rupture test rod with a diameter of 5mm. The axial direction of the test rod was parallel to the direction of the columnar crystal direction (that is, it was a longitudinal test rod).

The solid solution treatment temperatures used were 1100, 1150, 1170, 1190, 1210, 1230, 1250 and 1270°C. After each of the temperatures was maintained for 4 hours, it was air cooled and the rupture test rod underwent 900°C aging treatment for 16 or 32 hours after high temperature solid solution treatment.

The rupture tests were carried out on the BΠ-2 tester, we arranged a centigrade meter on a weight and measured the creep deformation of the test rod. The rupture and creep tests were carried out at 760°C under 73.8kgf/mm^2.

We used optical metallography and electron metallography to carry out structural analysis. We used concentrated ammonia water electrolytic erosion to display part of the structure and used a compound reagent of 12ml of H_3PO_4 + 47ml of H_2SO_4 + 41ml of HNO_3 for electrolytic erosion to display part of the structure.

We measured the size and volume fraction of the gamma-prime on an electron microphotograph and calculated the space of the gamma-prime phase particles. See Reference [6] for details on the measurement and calculation methods. The procedure was as follows:

1. We used several duplicate electron micrographs on different places of the specimen for each type of thermal treatment standard;

2. We measured the size a and volume fraction v_f of the gamma-prime on each photograph and used the mean value of the results obtained on the several photographs;

3. We calculated the center-to-center separation L and spacing λ of the average gamma-prime particles based on the formulas $L = \frac{a}{v_f^{1/3}}$ and $\lambda = a\left(\frac{1}{v_f^{2/3}} - 1\right)$.

In order to study the changes of the creep process' dislocation substructure and its interaction with the gamma-prime phase, we used a ~~transmision~~ SCANNING electron microscope to observe the thin film produced by the alloy after undergoing certain creep deformations (stages I, II and III). The creep tests /106 were carried out at 760°C under 73.8kgf/mm^2 (or 78kgf/mm^2) and 950°C under 25kgf/mm^2 conditions. The test was stopped when the creep deformation reached the preset requirement, it

was force cooled to room temperature when there was no loading and unloading and the structure of the creep state was frozen. We used a line cutting machine to cut thin alloy strips from the middle section of the test rod and the cutting direction and central axis of the test rod were 45° or perpendicular. We grinded the thin piece down to about 0.1mm and then made a thin film by means of double spray electroylsis polishing. The electroyltic liquid was a 10% perchlorate alcohol solution, the voltage was 40V, the temperature was controlled at about -20°C and the made thin film was placed in and observed with an H700 electron microscope. The electron microscope's operating voltage was 200kV.

III. Test Results

3.1 Changes of the Gamma-Prime Phase

Under casting conditions, the gamma-prime phase assumed a "田" shape and it was distributed on the entire base (Fig. 1a, see Plate 24). After solid solution treatment at 1100°C to 1270°C, the form and size of the gamma-prime phase underwent tremendous changes. Following the rise of the solid solution temperature, the cast state coarse gamma-prime phase gradually dissolved and during the cooling process we extracted using fine cubic shaped gamma-prime. The undissolved gamma-prime phase then continuously aggregated and grew. After solid solution treatment higher than 1210°C, the cast state coarse gamma-prime phase completely dissolved and the structure was completely composed of the fine cubic shaped gamma-prime phase. Figure 1 (see Plate 24) shows pictures taken by electron microscope after several types of solid solution temperature treatments. Figures 2 and 3 show the volume fraction v_f of the fine gamma-prime, particle size a (length of side of cube), the center-to-center separation L and interparticle spacing λ after various solid solution temperature treatments all of which were measured and calculated by the quantitative

metallographic method [6]. When the coarse and fine gamma-prime particles coexisted, it was necessary to deduct the volume of the coarse gamma-prime from the gamma-prime and calculate the volume fraction of the effective fine gamma-prime. We thus used this to calculate the L and λ of the fine gamma-prime.

图 1 γ′相形态的电子显微镜观察

Fig. 1 Morphology of γ′ phase in DSK3

(a) As-casted; (b) 1190°C, 4h+900°C, 32h;
(c) 1210°C, 4h+900°C, 32h;
(d) 1230°C, 4h+900°C, 32h;

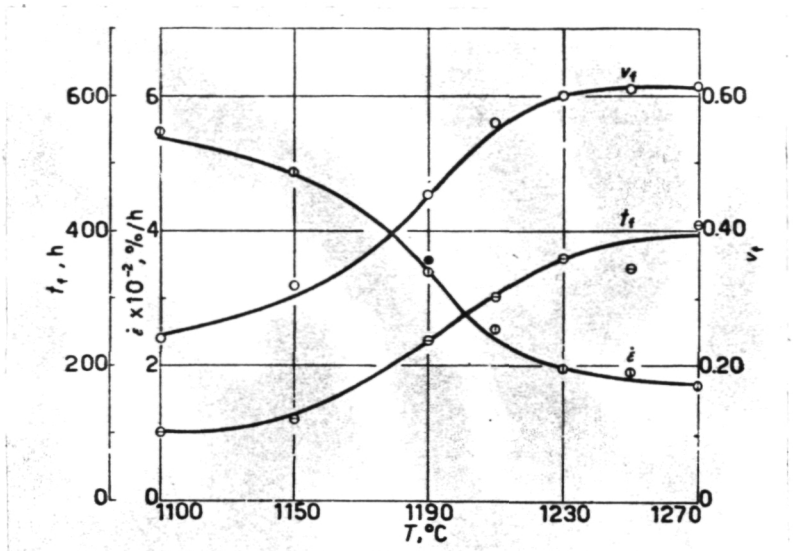

图 2 定向凝固 K3 合金细小 γ' 相体积分数 ν_f，持久寿命 t_f，第二阶段蠕变速率 $\dot{\varepsilon}$ 与固溶温度的关系

Fig. 2 Effect of solution temperature on the volume fraction, ν_f of γ', creep rupture life, t_f and secondary creep rate, $\dot{\varepsilon}$ at 760°C under 73.8kgf/mm²

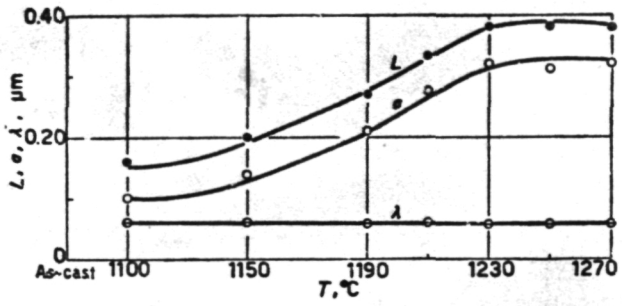

图 3 细小 γ' 尺寸 a，中心距 L，间距 λ 与固溶温度的关系

Fig. 3 Effect of solution temperature on the size, a centre-to-centre separation, L and interparticle spacing, λ of γ'

It can be seen from the figures that volume fraction /107
v_f of fine gamma-prime rises with the increases of the solid solution and the volume fraction basically did not change when it was over 1220°C because the structure was completely composed of the fine gamma-prime phase. The fine gamma-prime particles for the most part became cubic in shape, side length a and center-to-center separation L also increased with the rise of the solid solution temperature, a increased from 0.1μm at 1100°C to 0.23μm at 1230°C and interparticle spacing λ basically remained unchanged.

3.2 Rupture and Creep Performances

Following the raising of the solid solution temperature, the second stage creep rate $\dot{\varepsilon}$ of the alloy decreased when at 760°C under 73.8kgf/mm^2 and the life lengthened (Fig. 2). Rupture life t_f had the following relationship with second stage creep rate $\dot{\varepsilon}$ (Fig. 4.).

In the formula, a =1.02 ≒ 1, c=5.47 ≒ 5.5. It can be seen that the ~~rupture~~ FRACTURE life lengthened with the decrease of the second stage creep rate. /108

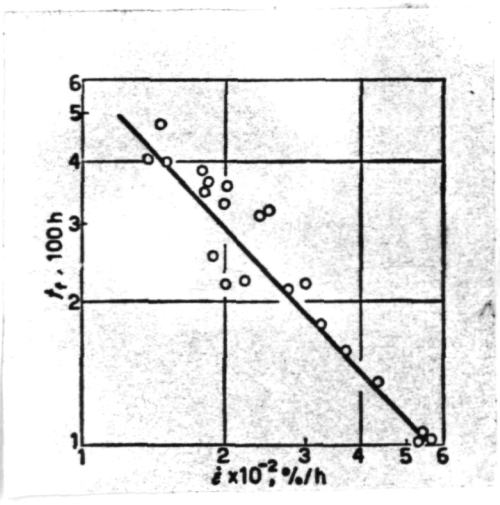

图 4 760°C, 73.8 kgf/mm² 下的持久寿命与第二阶段蠕变速率之间的关系

Fig. 4 Correlation between creep rupture life, t_f and secondary creep rate, $\dot{\varepsilon}$ at 760°C under 73.8 kgf/mm²

Second stage creep rate $\dot{\varepsilon}$ and rupture life t_f are related to effective volume fraction v_f of fine gamma-prime (see Fig. 5). It can be seen from the figure that the rupture life lengthened with the increase of the fine gamma-prime's volume fraction; the second stage creep rate decreased with the increase of the fine gamma-prime's volume fraction. It should be pointed out that while the gamma-prime's volume fraction changed, its size also changed and the rupture and creep performances of the alloy should be the result of the overall effects of the gamma-prime's volume fraction and size. After optimal solid solution treatment, the medium temperature rupture life was about 10 times higher than during the cast state.

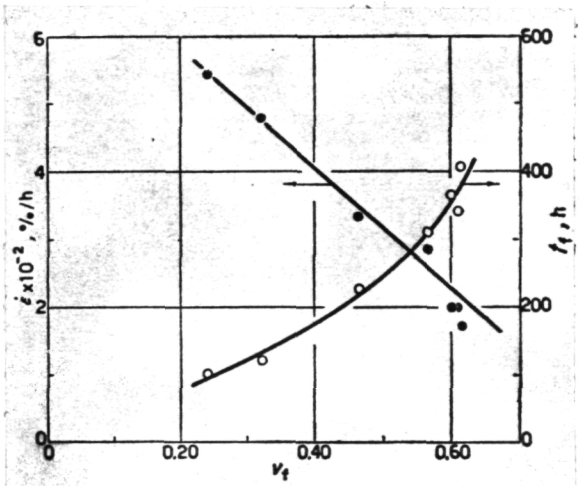

图 5 760°C, 73.8 kgf/mm² 下的持久寿命，第二阶段蠕变速率与细小 γ′ 体积分数的关系

Fig. 5 Correlation between creep rupture life, t_f at 760°C under 73.8 kgf/mm², secondary creep rate, $\dot{\varepsilon}$ and volume fraction, v_f of fine γ'

3.3 Changes of the Dislocation Substructure During the Creep Process

Before creeping, the alloy underwent 1210°C, 4h + 900°C, 32h treatment, the initial state of the gamma-prime particles

was square shaped and they were uniformly distributed. We can see from the TEM (Fig. 6, Plate 24) that the γ/γ' interface manifested a noticeable δ -type interface fringe. This is because the lattice parametric difference of the gamma and gamma-prime created tetragonal distortion in the base gamma of the γ/γ' interface area.

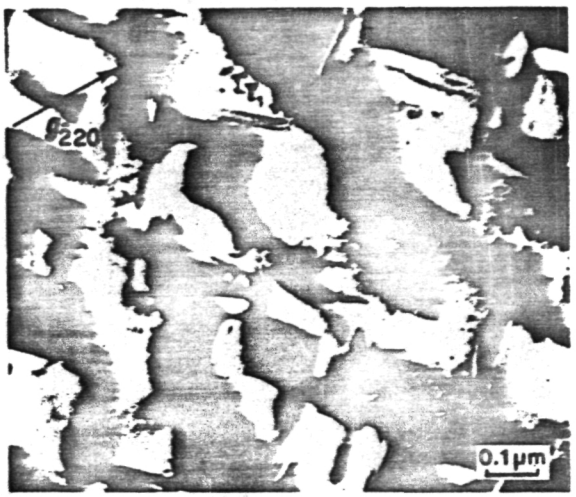

图 6 合金中γ′形态的电子衍衬图，γ/γ′界面呈现δ型条纹
Fig. 6 TEM of γ′ phase and δ-fringe appearing in γ/γ′ interface

After determination by X-ray, the direction of the columnar crystal axis was $\langle 100 \rangle$, γ' and γ had a cubic directional relationship, $\{100\}\gamma \parallel \{100\}\gamma'$ and $\langle 100 \rangle \gamma \parallel \langle 100 \rangle \gamma'$ and therefore the crystallographic direction of the creep test rods axis was $\langle 100 \rangle$. See Fig. 7 for the typical creep curves.

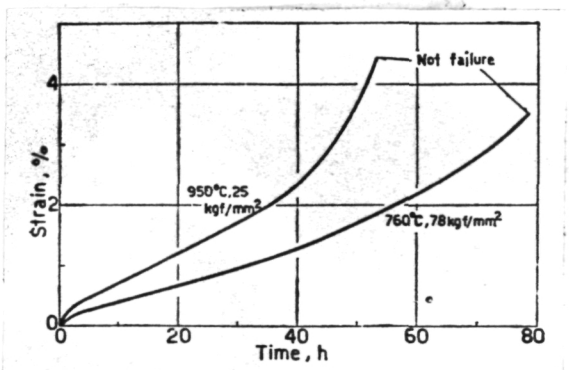

图 7 典型蠕变曲线图
Fig. 7 Typical creep curves

The 760°C creep process: during the primary stage of the creep process at 760°C under 73.8kgf/mm^2 or 78kgf/mm^2 the dislocation of the alloy could quite freely move on the gamma base between the gamma-prime. Figure 8 (Plate 25) shows the dislocated substructure of the typical primary stage creep process and because the spacing of gamma-prime was small therefore the distance the dislocation moved along the gamma base $\{111\}$ crystal face was only limited to spacing λ of the gamma-prime particles. It could be clearly observed that some of the slip movements of the two groups of parallel dislocation interconnections still had dislocation reactions. We did not observe any dislocations in the gamma-prime phase which shows that the dislocation was unable to cut across gamma-prime during the primary stage creep process. This was possibly due to the fact that the lattice parameter difference of the alloy's gamma and gamma-prime was relatively large. It caused the gamma-prime near the gamma/gamma-prime interface to possess a high eutectic strain field and prevented the dislocation from cutting across gamma-prime.

Following the increase of the creep distortion level, the dislocation density in the gamma base continually increased and when it entered into the second creep stage, the production and loss rate of dislocation were equal. This caused the dislocation density in gamma to remain unchanged. The typical dislocation substructure of the second stage of creeping is as shown in Fig. 9 (see Plate 26). High density irregular three-dimensional dislocated lattice formed in the gamma base, we observed a small number of dislocations in the gamma-prime under the high stress of 78kgf/mm^2 and they appeared in pairs. This signified that a small number of dislocations cut across the gamma-prime phase with superlattice structure. We did not observe dislocations in the gamma-prime phase when the face was under relatively the low stress of 73.8kgf/mm^2. Reference [6] pointed out that the Burger vector of the dislocation pairs is $a/2\langle 110\rangle$. Figure 10 (see Plate 26) shows the dislocation

substructure of the third stage of creeping, the characteristics are similar to those of the second stage only the dislocation density was a little higher.

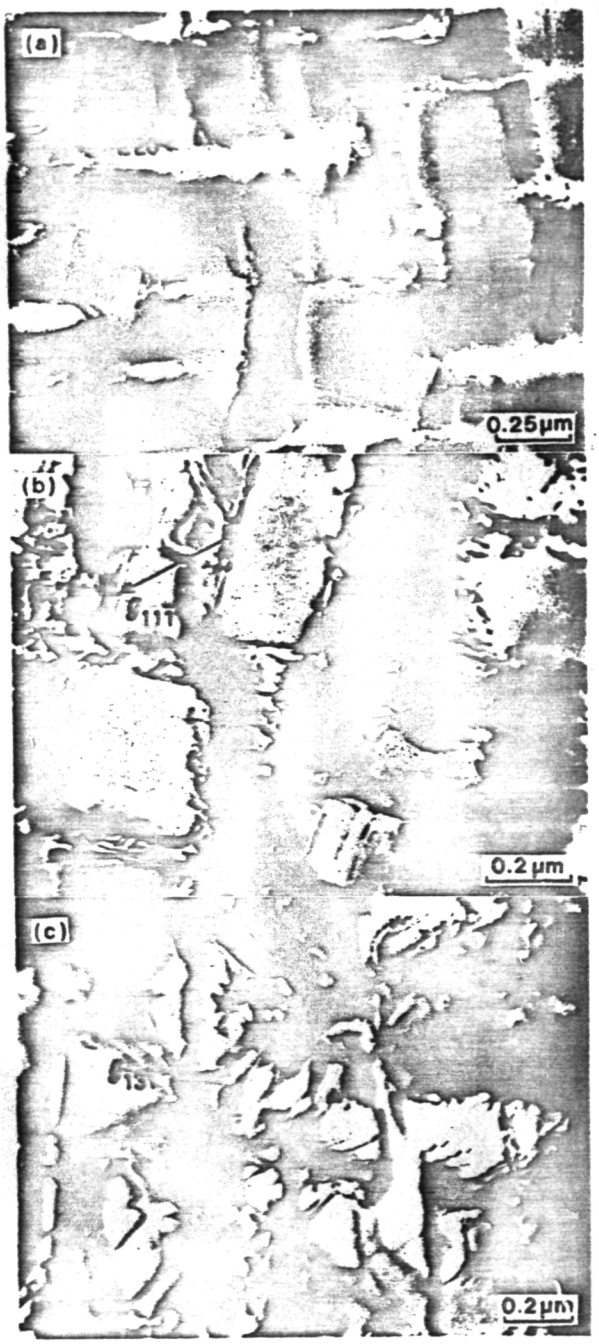

图 8 760°C第一阶段蠕变过程的位错亚结构

Fig. 8 Dislocation structure and γ' morphology during primary creep
(a), (b) 760°C, 78kgf/mm², 2h, δ=0.16%;
(c) 760°C, 73.8kgf/mm², 2h, δ=0.30%

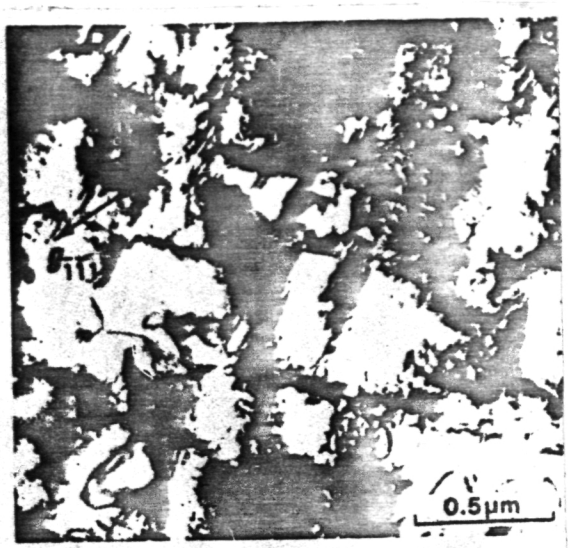

图 9 蠕变第二阶段位错亚结构的电子衍衬象
Fig. 9 TEM of dislocation structure during secondary creep to δ=1.1% at 760°C under 78kgf/mm², 30h

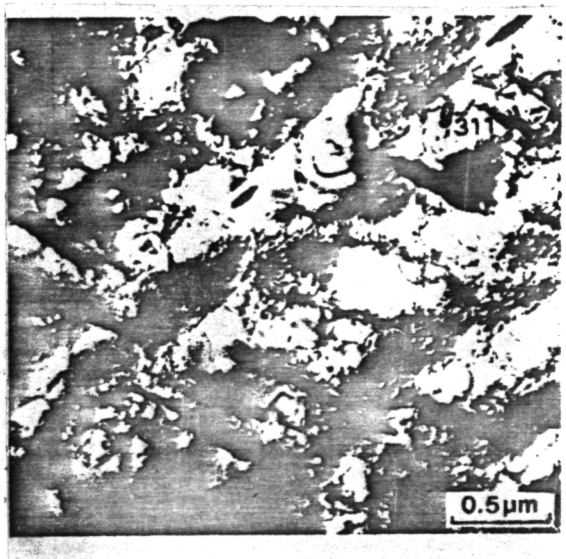

图 10 蠕变第三阶段位错亚结构的电子衍衬象
Fig. 10 TEM of dislocation structure during tertiary creep to δ=3.36% at 760°C under 78kgf/mm² 78h

Based on the above observation results, it was very difficult for the dislocations to cut across gamma-prime during the 760°C creep process. Most of the dislocations accumulated in the high density three-dimensional dislocation lattice which formed in the gamma base, the slip of the dislocations was limited by them and thus raised the creep resistance. When the dislocation only went through climbing, the contrary sign dislocations met and were lost which /109 decreased the dislocation density. This caused the three-dimensional dislocation network in the gamma base to become loose, it lengthened the side length of the network, lowered the stress which started the dislocations and thus enabled the dislocations to further slip and proliferate in the gamma base and produce new dislocations. The production and loss rates of dislocations during the second stage creep process were equal and the dislocation density ρ in the alloy remained unchanged.

The 950°C creep process: at 950°C, the morphology and size of gamma-prime changed with the creep process. This was especially the case during the later period of the second stage and during the third stage when the gamma-prime became coarse and assumed a long strip shape. At 950°C, during the initial period of the first stage of creeping of the alloy, the dislocation substructure was similar to that during 760°C creeping (Fig. 11, see Plate 26) and yet the two groups of dislocations easily produced reactions and formed a two-dimensional dislocation network in the area of the γ/γ' interface. During the second stage of creeping, the gamma-prime became coarse and assumed a long strip shape. The dislocation density in the gamma base was lower than at 760°C, a two-dimensional dislocation network appeared in the γ/γ' interface area (Fig. 12, see Plate 26) and gamma-prime had already become coarse and assumed a long strip shape.

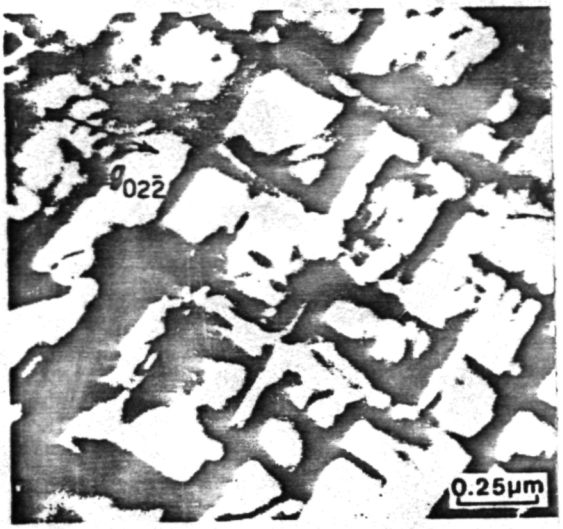

图 11 蠕变第一阶段位错亚结构的电子衍衬象
Fig. 11 TEM of dislocation structure during primary creep to δ=0.42% at 950°C under 25kgf/mm², 2h

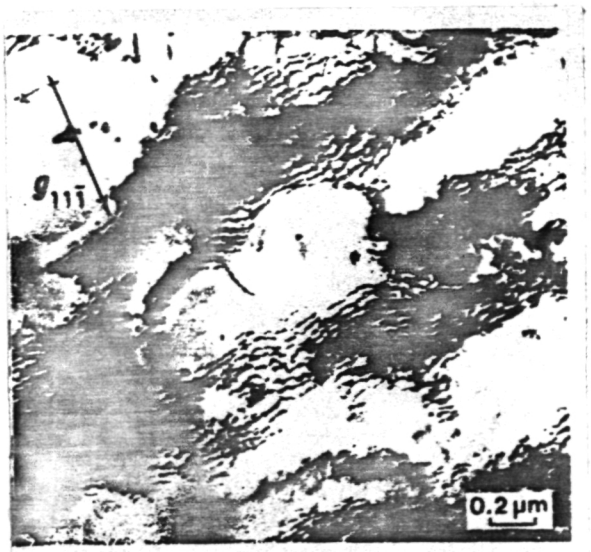

图 12 蠕变第二阶段位错亚结构的电子衍衬象
Fig. 12 TEM of dislocation structure during secondary creep to δ=1.37% at 950°C under 25kgf/mm², 20h

IV. Discussion

During the high temperature creep process, the high strength nickel base-superalloy which used gamma-prime as the strengthening phase have dislocations which slip in the gamma base and are obstructed in the periphery of gamma-prime. It was necessary to cause the alloy to continuously produce creep distortion and the dislocations had to continuously slip based on the following three methods of overcoming obstructions:

(1) Cut gamma-prime and go through; (2) bend between the gamma-prime and revolve around the gamma-prime (Orowan model); (3) climb and go past the gamma-prime.

As regards the alloy studied in this paper, the volume fraction of the gamma-prime reached 0.63, after solid solution treatment the side length of the fine square gamma-prime was only 0.2-0.3μm and its spacing was very small, about 0.05-0.07μm. Within the stress range used in this test, we did not observe traces of dislocations cutting gamma-prime during the first stage of the creep process and the dislocations only moved along the gamma base path between the gamma-prime (Fig. 8). In order to maintain the continuity of the specimen during the distortion process, it was necessary to not have the $\frac{a}{2}\langle 110\rangle$ dislocation of one group slip and move on the $\{111\}$ face of the gamma base. We could generally observe that the dislocations of the two groups of $\frac{a}{2}\langle 110\rangle$ Burgers vectors produced dislocation reaction when they intersected and a dislocation network was formed (irregular or regular). Following the increase of the deformation level, the dislocation density increased, the size of the network became smaller and the creep rate slowed down. When the creeping reached the second stage, the dislocation density in the gamma base remained constant. Under medium temperature (760°C), the dislocation density was relatively high and the network was more irregular. Under high

temperature (950°C), however, a more regular dislocation network formed. The applied stress was relatively low when there was high temperature creeping and thus the dislocation density was also relatively low.

The second stage creeping can be seen as the result of the recovery and work hardening dynamic state equilibrium. We can derive the Bailey-Orowan equation [7,8] from recovery rate $r = \frac{\partial \sigma i}{\partial t}$ and work harding coefficient $h = \frac{\partial \sigma i}{\partial \varepsilon}$:

$$\dot{\varepsilon} = \frac{r}{h} \qquad (2)$$

In this equation, σ_i is the mean internal stress in the material. D. McLean [9] pointed out that the dislocation density in the alloy and the distribution state are the major factors /110 which determine its being able to endure external force. As regards pure metals, recovery causes the dislocation network to become loose by means of dislocation climbing, it lengthens the side length of the network and decreases the stress which begins dislocations. Therefore, the dislocations can further the slipping and proliferation in the gamma base and produce new dislocations. During the second stage creep process, the production and loss rate of dislocations were equal and the dislocation density of the alloy did not change.

The second stage creep rate was limited by the climbing and slipping processes of the dislocations and the one with the slow process rate was the controlling factor of the creep rate. Reference [10] pointed out that during the high temperature (850°C) second stage creep process, a dislocation network wall formed on the gamma/gamma-prime interface of a nickel-base superalloy and the climbing of the edge location on the wall was the controlling factor of the high temperature creeping; the slipping of the dislocation produced creep deformation and the new dislocation stage replenished the dislocations lost during recovery. This agrees with the dislocation substructure observed after creeping of the alloy at 950°C under

under 25kgf/mm^2 studied in this paper. However, after the second stage of creeping at 760°C under 73.8kgf/mm^2 or 78kgf/mm^2, the network dislocations will not only produce climbing near the gamma/gamma-prime interface and between the gamma-prime but the slipping movements of the dislocations will also be obstructed by the dislocation network.

The morphology, size and number of the gamma-prime employ the following two production effect results which influence the creep performance. One is the changing of the dislocation density and composition in the gamma base as well as the level of freedom of the dislocation slip movement. The other affects the recovery process, that is, it affects the climbing process of the dislocation. Based on the method of analysis in Reference [6], we began from the dislocation climbing model and were able to establish the second stage creep process. During the second stage of creeping, creep rate $\dot{\varepsilon}$ could be given by the following formula:

$$\dot{\varepsilon} = NabR \qquad (3)$$

In the formula, N is the dislocation source volume density. It is the dislocation source number of the edge type dislocations in the unit volume which can climb past the gamma-prime particles or the dislocation source number of the nodal point spacing which reaches startable length l_s after the network after the network goes through climbing in the unit volume. A is the sweeping area after the dislocation source begins and b is the magnitude of the Burgers vector of the dislocation. R is the rate of the dislocation passing the gamma-prime particles or the rate that the network nodal point spacing reaches l_s, that is, the quantity of dislocation source which starts in the unit time.

The relationship of N with movable dislocation density ρ_m and source dislocation length l_s is:

$$N = \rho_m / l_s \qquad (4)$$

l_s and the dislocation network's mean nodal point spacing $\bar{l}$ form a certain ratio:

$$l_s = m\bar{l} \tag{5}$$

Kuhlman-Wilsdorf pointed out: m=3[11]:

$$N = \rho_m / m\bar{l} \tag{6}$$

Moreover, $\bar{l} = 1/\sqrt{\rho}$. Under creeping conditions, the relationship between dislocation total density ρ of the alloy and applied stress σ accord with the following relational formula:

$$\sigma - \sigma_o = \alpha Gb\sqrt{\rho} \tag{7}$$

In the formula, G is the shear modulus, b is the magnitude of the Burgers vector of the dislocation, a is the proportional constant and σ_o are all of the other causes which contribute to flow stress (lattice resistance, base solid solution str engthening and second phase strengthening etc.) other than the dislocation-dislocation interaction.. Under creeping conditions we take [12]

$$\rho_m = \alpha_e (\sigma - \sigma_o)^{\beta} \tag{8}$$

In the formula, α_e and β are separately the proportional constant and exponent and the value of β is taken as $\beta = 0-1$[12]. We substituted formulas (7) and (8) into formula (6) and obtained: /111

$$N = \frac{\alpha_e}{m\alpha^3 G^3 b^3} (\sigma - \sigma_0)^{3+\beta} \tag{9}$$

It is different from the alloy used in Reference [6]. The gamma-prime phase spacing of this alloy was relatively small and the distribution was only limit ed to the movement in the λ dimension range. The edge dislocations on the surrounding dislocation network wall of the gamma/gamma-prime interface had the following sweep area after climbing past the gamma/gamma-prime particles:

$$A = \lambda^2 \tag{10}$$

When the distribution of the base gamma between the gamma-prime also had a dislocation network, A was smaller than λ^2, that is:

$$A=a_a\lambda^2 \tag{11}$$

a_a is the proportional constant which is less than 1.

When there were no stop volume dislocation circles around the second phase particles, Ansell and Weertman [13] gave the rate that the dislocation passes the gamma-prime particles as:

$$R=\frac{\sigma_i b^2 D}{HkT}=\frac{(\sigma-\sigma_0)b^2D}{HkT} \tag{12}$$

In the formula, σ_i is the internal stress added on the climb dislocation, k is the Boltzman constant, T is the absolute temperature, D is the bulk diffusion coefficient and H is the climb distance required by the dislocation to climb past gamma-prime. In this study,

$$H=a_c a \tag{13}$$

a_c is the proportional constant and a is the dimension of gamma-prime (the side length of the cube). When we substituted formulas (9), (11), (12) and (13) and $D=D_o\exp(-Q_s/RT)$ into (3), we obtained:

$$\dot{e}=\frac{K}{G^3T}\frac{\lambda^2}{a}(\sigma-\sigma_0)^n\exp(-Q_s/RT) \tag{14}$$

In this formula, $K+\frac{a_e a_a D_o}{m a_c a^3 k}$, $n=4+\beta$, $\beta=0-1$ and therefore n=4-5. We took the relationship of the gamma-prime particle's volume fraction v_f and the particle's side length to be $\lambda=a\left(\frac{1}{v_f^{1/3}}-1\right)$ and obtained /112

$$\dot{e}=\frac{K}{G^3T}\frac{a}{v_f^{1/3}}(1-v_f^{1/3})^2(\sigma-\sigma_0)^n\exp(-a_s/RT) \tag{15}$$

When there were fixed temperature and stress, $\dot{\varepsilon}\propto\lambda^2/a$ or $\dot{\varepsilon}\propto\frac{a}{v_f^{2/3}}(1-v_f^{1/3})^2$ and if we arranged the data of size a of

fine gamma-prime of different solid solution temperature (900°C, 32h aging) processing, effective volume fraction v_f, the spacing λ value and second stage creep rate $\dot{\varepsilon}$ at 760°C under 73.8kgf/mm^2 into the relational chart of $\dot{\varepsilon} - \lambda^2/a$ or $\dot{\varepsilon} - \frac{a}{v_f^{2/3}}(1-v_f^{1/3})^2$ we could obtain a linear relationship (see Figs. 13 and 14) which agreed with the theoretically reduced relational formula.

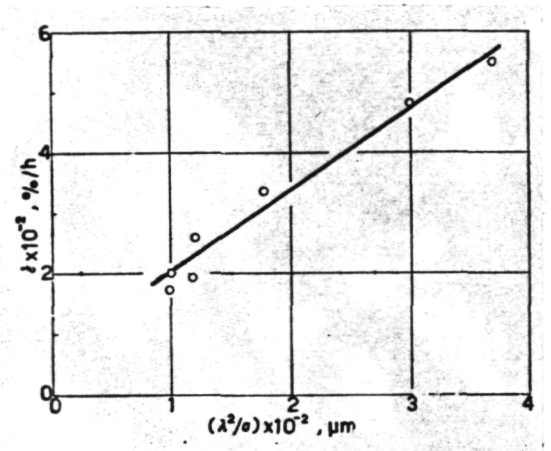

图 13 第二阶段蠕变速率与 λ^2/a 的关系

Fig. 13 Correlation between secondary creep rate, $\dot{\varepsilon}$ and λ^2/a

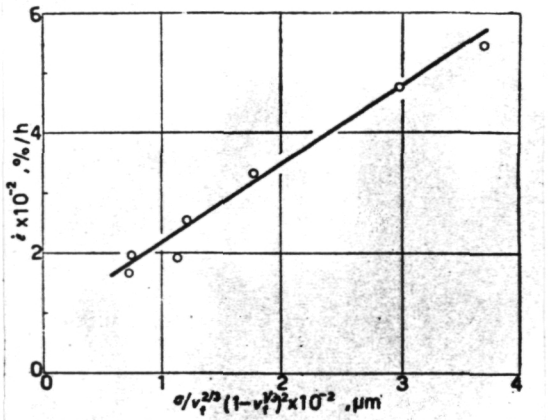

图 14 第二阶段蠕变速率与 $\frac{a}{v_f^{2/3}}(1-v_f^{1/3})^2$ 的关系

Fig. 14 Correlation between secondary creep rate, $\dot{\varepsilon}$ and $\frac{a}{v_f^{2/3}}(1-v_f^{1/3})^2$

V. Conclusions

1. In the 1100-1270°C temperature range, the volume fraction of fine gamma-prime in the alloy increased with the increase of the solid solution temperature and the size of the fine gamma-prime also enlarged along with it.

2. Suitable high temperature solid solution accompanied by 900°C aging processing was able to raise the medium temperature (760°C under 73.8kgf/mm^2) rupture life of the directionally solidified alloy about 10 fold.

3. The medium temperature creep performance of the alloy was determined by volume fraction v_f of fine gamma-prime, size a of gamma-prime (the side length of the cube) and spacing λ of gamma-prime agreeing with the relationship $\dot{\varepsilon} \propto \lambda^2/a$ or $\dot{\varepsilon} \propto \frac{a}{v_f^{2/3}} (1-v_f^{1/3})^2$ under fixed temperature and stress.

References

[1] VerSnyder, F.L.: Shank, M.E., Mater.Sci.Eng.,6(1970),213.

[2] Lin Dongliang and Yao Deliang, Journal of Metallurgy, 15(1979), 177.

[3] Lin Dongliang and Wang Laisheng, Study of the Directionally Solidified Nickel-Base Cast Superalloy K17G, (unpublished).

[4] Lin Dongliang, Yao Deliang, Cai Bingchu, Sun Chuanqi and Zhou Baozhu, Mechanical Engineering Materials,(1979),No.5,1.

[5] Jackson, J.J.; Donachie, M.J., Henricks,R.J.; Gell,M., Metall.Trans.,8A(1977),1615.

[6] Lin Dongliang,Journal of Metallurgy,17(1981),26.

[7] Bailey,R.W., J.Inst.Met.,35(1926),27.

[8] Orowan,E.,West Scot Iron Steel Inst.,54(1946-47),45.

[9] McLean,D.Rep.Prog,Phys.,29(1966),1.

[10] Carry,C.; Strudel, J.L.,Acta Metall.,26(1978),859.

[11] Kuhlmann-Wilsdorf,D., Metall.Soc.Conf.,Vol.46,Work Harding, Eds.Hirth,J.P.;Weertman,J.Gordon and Breach,NY 1968,p.97.

[12] Orlova,A.,Scr.Metall.,13(1979),763.

[13] Ansell,G.S.;Weertman,J.,Trans.Metall.Soc.AIME,215(1959),838.